Estrogen 17β-estradiol accelerates the proliferation of uterine junctional zone smooth muscle cells via the let-7a/Lin28B axis in adenomyosis

JUN-HUA HUANG, HUA DUAN, SHA WANG and YI-YI WANG

Department of Minimally Invasive Gynecology Center, Beijing Obstetrics and Gynecology Hospital, Capital Medical University, Beijing 100006, P.R. China

Received September 14, 2020; Accepted February 12, 2021

DOI: 10.3892/mmr.2021.11976

Abstract. The estrogen 17β-estradiol has been proven to serve an indispensable role in the occurrence and development of adenomyosis (ADS). The let-7a/Lin28B axis can control cell proliferation by acting as a tumor-inhibiting axis in numerous types of cancer. However, its role in ADS remains unknown. The present study aimed i) to elucidate the role of let-7a in regulating the proliferation of human uterine junctional zone (JZ) smooth muscle cells (SMCs) in ADS, ii) to evaluate whether 17β-estradiol modifies the expression levels of let-7a and Lin28B in JZ SMCs in ADS, and iii) to establish how 17β-estradiol affects the function of the let-7a/Lin28B axis in the proliferation of JZ SMCs in ADS. A total of 36 premenopausal women with ADS were enrolled as the experimental group and 34 women without ADS were recruited as the control group. Reverse transcription-quantitative PCR was used to evaluate the expression level of let-7a, and western blotting was performed to determine the Lin28B expression levels. Lentiviral null vector, let-7a overexpression lentiviral vector GV280 and let-7a inhibition lentiviral vector GV369 were used to infect cells to alter the expression of let-7a for further functional experiments. 17β-estradiol and Cell Counting Kit-8 assays were conducted to determine how 17β-estradiol affects the function of the let-7a/Lin28B axis in the proliferation of JZ SMCs in ADS. The results demonstrated that let-7a was downregulated and Lin28B was upregulated in the JZ SMCs of ADS compared with the control cells ($P<0.0001$). Moreover, a lower expression of let-7a led to faster proliferation of JZ SMCs ($P<0.05$), and 17β-estradiol affected the let-7a/Lin28B axis to accelerate the proliferation of JZ SMCs in ADS ($P<0.05$). These data suggested that 17β-estradiol collaborates with the let-7a/Lin28B axis to affect the development of ADS.

Correspondence to: Professor Hua Duan, Department of Minimally Invasive Gynecology Center, Beijing Obstetrics and Gynecology Hospital, Capital Medical University, 17 Qi Helou Road, Dong Cheng, Beijing 100006, P.R. China
E-mail: duanhua@ccmu.edu.cn

Key words: adenomyosis, 17β-estradiol, let-7a, Lin28B, proliferation, junctional zone

Introduction

Adenomyosis (ADS) is an estrogen-dependent disorder (1) that disturbs the fertility of reproductive-age women. A recent 10-year (2006-2015) population-based cohort study in the United States showed a 1% incidence of ADS among women aged 16-60 years (2). This condition involves endometrial stroma and glands present in the myometrium of the uterus (3), which lead to a series of clinical symptoms, including progressive dysmenorrhea, abnormal uterine bleeding and subfertility. Although this condition has been recognized for >100 years (4), its etiology and pathogenesis are yet to be fully elucidated.

The width of junctional zones (JZs) on T2-weighted images is the main diagnostic factor of ADS (5). Disturbed uterine JZs generate inordinate peristalsis and impaired uterotubal transport, which may contribute to the development of ADS (6,7). Some studies have indicated that abnormal uterine contractions that originate exclusively from JZs (8) may be a cause of dysmenorrhea (9). Gonadotropin-releasing hormone analogs have been reported to reduce the width of JZs (10,11), indicating that estrogen may regulate the hyperplasia and hypertrophy of JZ smooth muscle cells (SMCs) to some extent (12). Our previous studies also revealed that compared to the outer myometrium, there are more organelles on the ultrastructure in myocytes of the JZ (13), and that estrogen can accelerate SMC proliferation in the JZs of the uterus, which affects JZ contraction (14,15) . In addition, accumulating evidence has shown that hyperestrogenism in ADS is similar to that in uterine wound repair (16). It has been reported that estrogen receptor α (ERα) can regulate oxytocin (OT) and OT receptor (OTR) to induce peristalsis in the uterine myometrium (17). When OTR is upregulated in the myometrium of ADS, uterine peristalsis is also active (8). If tissues in the JZ are injured, inflammation and a series of cascade reactions will occur. First, elevated IL-1β expression induces cyclooxygenase-2 (COX-2) to produce prostaglandin E2 (PGE2). Second, P450 aromatase level is increased, which in turn upregulates steroidogenic acute regulatory protein (StAR). Finally, StAR induces estradiol to augment the expression of estrogen receptor β (ERβ), which then accelerates the development of ADS (18-20).

MicroRNAs (miRNAs/miRs) are non-coding RNAs that serve a critical role in post-transcriptional gene regulation (21).

miR-let-7 is one of the most studied miRNAs and includes several variants: let-7a, let-7b, let-7c, let-7d and let-7e (22). Lin28 is an RNA-binding protein that can bind to the RNA-binding domains of let-7 to control cellular function (23). There are two homologous members in the Lin28 family, Lin28A and Lin28B, and their expression levels are negatively correlated with let-7 (24). Several studies have reported that the let-7/Lin28 axis regulates pluripotency, reprogramming and tumorigenicity in various diseases (25-28), including neurodegenerative diseases (28), oral squamous carcinoma (29), breast cancer (30) and lung cancer (31). Therefore, this axis may modulate the proliferation and differentiation of normal and abnormal cells. Some studies have revealed that women with endometriosis have several miRNAs (let-7b, miR-135a, let-7c, let-7d, let-7e and let-7f) that are differentially expressed in sera or cells (32,33). Moreover, our previous study found that let-7a was negatively correlated with Lin28B expression in the JZ in ADS (34).

Based on the aforementioned findings, we hypothesized that 17β-estradiol may affect the let-a/Lin28B axis to regulate the proliferation of JZ SMCs, resulting in disordered JZ contraction and a series of clinical symptoms of ADS. Therefore, the present study was designed with the following aims: i) To study how let-7a regulates the proliferation of uterine JZ SMCs in ADS; ii) to determine whether 17β-estradiol can change the let-7a/Lin28B axis expression level to accelerate the development of ADS; and iii) to establish how 17β-estradiol affects the function of the let-7a/Lin28B axis in the proliferation of JZ SMCs in ADS.

Materials and methods

Sample collection and cell primary culture. This study was approved by the Ethical Committee of Clinical Research of Beijing Obstetrics and Gynecology Hospital, Capital Medical University, China (reference no. 2016-KY-012), and conducted according to the Declaration of Helsinki. Between July 2019 and January 2020 at the Beijing Obstetrics and Gynecology Hospital, 36 patients diagnosed with ADS were enrolled as the experimental group and 34 patients diagnosed with early-stage cervical cancer, early-stage ovarian cancer or uterine prolapse without ADS were recruited as the control group. All of these individuals (age, 30-50 years) were premenopausal women with regular menses before the hysterectomy operation (lengths ranging between 21 and 35 days). The inclusion criteria for the experimental group was patients aged 30-50 years diagnosed with ADS that had undergone a hysterectomy. in the inclusion criteria for the control group was patients diagnosed with early-stage cervical cancer, early-stage ovarian cancer or uterine prolapse, who had undergone a hysterectomy. The exclusion criteria included endometriosis, endometrial polyps, fibroids, pelvic inflammation, endometrial and myometrial cancer, use of hormones or intrauterine devices within 3 months before surgery, and preoperative radiotherapy and chemotherapy. All patients signed informed consent before the hysterectomy. After the surgery, pathological examination was used to determine if there were also other uterine pathologies.

After the uterus was removed, it was opened immediately in a Y shape and multiple 5 mm^3 samples were acquired from the JZ (underneath the endometrium) and then placed in saline solution at 4˚C for laboratory cell culture. The tissues from the JZ were cut into small pieces and digested with collagenase type II powder (cat. no. 17101015; Gibco; Thermo Fisher Scientific, Inc.) and DNase I (cat. no. EN0521; Gibco; Thermo Fisher Scientific, Inc.) for 4-5 h at room temperature. Then, after filtration and centrifugation(1,200 x g, 25˚C, 10 min), the cells were incubated in DMEM with 15% FBS (Biological Industries) at 37˚C in a 5% CO_2 incubator for subsequent experiments. Due to bacterial or fungal infection, there were only 20 ADS tissues that successfully produced primary cells and were used for subsequent cell functional experiments.

RNA extraction and reverse transcription-quantitative PCR (RT-qPCR). Total RNA was extracted from 20 ADS samples and 20 control samples according to the manufacturer's instructions for RNAiso Plus (cat. no. 9108; Takara Bio, Inc.), and its quality and quantity were assessed on a NanoDrop 2000/2000c Spectrophotometer (Thermo Fisher Scientific, Inc.). Then, for Lin28B detection, RT (37˚C for 1 h, followed by termination at 85˚C for 5 min in a thermal cycler)and qPCR (initial denaturation: 95˚C for 10 sec, followed by 40 cycles of denaturation at 95˚C for 10 sec, annealing and elongation at 60˚C for 20 sec) were performed using PrimeScript RT reagent kit with gDNA Eraser (cat. no. RR047A; Takara Bio, Inc.) and SYBR Premix Ex Taq II (Tli RNase H Plus; cat. no. RR820A; Takara Bio, Inc.), respectively, on an ABI 7500 Real-Time PCR system (Applied Biosystems; Thermo Fisher Scientific, Inc.). For let-7a detection, Mir-X miRNA First-Strand Synthesis kit (cat. no. 638313; Takara Bio, Inc.) was used for RT (37˚C for 1 h, followed by termination at 85˚C for 5 min in a thermal cycler) and TB Green Advantage qPCR Premix (cat. no. 639676; Takara Bio, Inc.) was used for qPCR. Two-step qPCR was used for let-7a detection, as follows: Initial denaturation for 30 sec at 95˚C, followed by 40 cycles of denaturation at 95˚Cfor 5 sec, and annealing and elongation at 60˚C for 34 sec. Dissociation curve analysis was conducted at 95˚C for 60 sec, 55˚C for 30 sec and 95˚C for 30 sec. The $2^{-\Delta\Delta Cq}$ method was used to examine the relative expression levels of let-7a and Lin28B (35). Since the Mir-X miRNA First-Strand Synthesis kit supplied the mRQ 3' primer as the 3' primer for let-7a detection in qPCR, the entire sequence of mature let-7a was used as the miRNA-specific 5' primer. The primer specific for let-7a was 5'-CCGCGCGCGCTAT ACAATCTACTGTCT-3', and U6 was used for normalization with these primers: Forward, 5'-AACGAGACGACGACAGAC-3' and reverse, 5'-GCAAATTCGTGAAGCGTTCCATA-3'. The primers used for Lin28B were forward, 5'-AACCAGGTTTCA TCAGCCCC-3' and reverse, 5'-ACTTACAGTGGCCAGTT CCG-3'; and GAPDH was used as an internal control with the following primers: Forward, 5'-CTCCTCCACCTTTGACG CTG-3' and reverse, 5'-TCCTCTTGTGCTCTTGCTGG-3'.

Western blotting. RIPA buffer (cat. no. R0010; Beijing Solarbio Science & Technology Co., Ltd.) was used to lyse cells and extract total protein from 20 ADS samples and 20 control samples, a protease inhibitor cocktail (cat. no. P8340; Sigma-Aldrich; Merck KGaA) was added to inhibit the degradation of proteins. The protein concentration was measured using an Enhanced BCA Protein Assay kit (cat. no. P0010; Beyotime Institute of Biotechnology). Then, 10% SDS-PAGE (cat. no. D1060; Beijing Solarbio Science & Technology Co., Ltd. was used for electrophoresis, and the protein was transferred to PVDF membranes (cat. no. IPVH00010;

EMD Millipore). The membranes were blocked for 2 h at room temperature with 5% non-fat dry milk. Rabbit monoclonal anti-Lin28B (1:500; cat. no. ab191881; Abcam) and rabbit polyclonal anti-α tubulin (1:2,000; cat. no. AC007; ABclonal Biotech Co., Ltd.) were added to the membranes and incubated at 4˚C with gentle agitation overnight. Finally, the membranes were washed three times using Tris-buffered saline-Tween-20 (cat. no. T1085; Beijing Solarbio Science & Technology Co., Ltd.) and incubated with HRP goat anti-rabbit IgG (1:5,000; cat. no. AS029; ABclonal Biotech Co., Ltd.) for 1 h with gentle agitation at room temperature. Immunoreactive bands were detected using Chemiluminescent HRP Substrate (cat. no. WBKLS0500; EMD Millipore). ChemiDoc TM XRS+ and Image Lab software 3.0 (Bio-Rad Laboratories, Inc.) were used to collect imaging information.

Cell treatments. Primary cells were starved for 24 h and exposed to 17β-estradiol (10 nmol/l; cat. no. 3301; Sigma-Aldrich; Merck KGaA) or dimethyl sulfoxide (DMSO; cat. no. 276855; Sigma-Aldrich; Merck KGaA) as the control group for 24 h at 37˚C. 17β-estradiol was dissolved in the DMSO.

Transfection. The empty lentiviral vector (Shanghai Genechem Co., Ltd.) was used to infect the ADS group as the control for both let-7a overexpression and inhibition, the let-7a overexpression lentiviral vector GV280 (hU6-MCS-Ubiquitin-EGFP-IRES-puromycin; Shanghai Genechem Co., Ltd.) was used to infect the ADS group as the Lenti-GV280 group , and the let-7a inhibition lentiviral vector GV369 (Ubi-MCS-SV40-EGFP-IRES-puromycin; Shanghai Genechem Co., Ltd.) was used to infect the ADS group as the Lenti-GV269 group. Lentiviral vector was mixed with DMEM (Biological Industries) and infected into the cells at a multiplicity of infection of 10 ($1x10^7$ TU/ml) for 12 h at 37˚C after cells were grown to a density of 30-40%. After 72 h, transfection efficiency was observed using white light microscopy and fluorescence microscopy. Subsequently, the cells were selected using 1 μg/ml puromycin (cat. no. P8230; Beijing Solarbio Science & Technology Co., Ltd.) until there were no dead cells in the culture plates. Transfected cells were used for western blotting, RT-qPCR and cell functional assays.

Cell Counting Kit (CCK)-8 assays. A total of 1,000 JZ SMCs/well were seeded in 96-well plates and incubated at 37˚C in 5% CO_2. Then, CCK-8 solution (10 μl; cat. no. CK04; Dojindo Molecular Technologies, Inc.) was added to each well at different time points (12, 24, 36, 48, 60, 72, 84 and 96 h) and incubated for 4 h at 37˚C, according to the manufacturer's instructions. Finally, the absorbance was measured at 450 nm on a microplate reader

Statistical analysis. GraphPad Prism 8.4 (GraphPad Software, Inc.) was used for data analysis. All normally distributed data are presented as the mean ± SD. Unpaired Student's t-test or Wilcoxon signed-rank test were used to compare differences between two groups. One-way ANOVA was used to compare ≥3 groups. When means were significantly different from each group as determined by ANOVA least significant difference and Student-Newman-Keuls post hoc tests were conducted. P<0.05 was considered to indicate a statistically significant difference.

Results

let-7a controls the expression of Lin28B in JZ SMCs. RT-qPCR results demonstrated that let-7a was downregulated (Fig. 1A) and Lin28B (Fig. 1B) was upregulated in ADS JZ SMCs compared with the control JZ SMCs (both P<0.0001). Western blot analysis also verified that the expression level of Lin28B was higher in the ADS group compared with in the control group (P<0.0001; Fig. 1C and D).

To further examine the relationship between let-7a and Lin28B, let-7a was overexpressed and knocked down to examine its effect the expression of Lin28B in the JZ SMCs of the ADS group via RT-qPCR and western blotting. Fluorescence microscopy and RT-qPCR were used to verify the transfection efficiency of the let-7a overexpression lentiviral vector GV280 and the let-7a inhibition lentiviral vector GV369 (Fig. 2). The results demonstrated that when let-7a was overexpressed, Lin28B was downregulated; when let-7a was downregulated, the expression of Lin28B was upregulated (Fig. 3). Thus, it was suggested that let-7a controlled the expression of Lin28B in JZ SMCs.

Low expression of let-7a leads to high proliferation of JZ SMCs. JZ SMCs transfected with the lentiviral null vector, let-7a inhibition lentiviral vector GV369 and let-7a overexpression lentiviral vector GV280 were used to investigate how let-7a participated in the initiation and development of ADS. The CCK-8 results demonstrated that the lenti-GV280 cells had a significantly lower 450 nm absorbance value compared with the lenti-NC cells after 36 h (P<0.05; Fig. 4A), while the lenti-GV369 cells had a higher 450 nm absorbance value after 48 h (P<0.05 Fig. 4B). Therefore, low expression of let-7a could accelerate the proliferation of JZ SMCs in ADS.

Treatment with 17β-estradiol affects the expression of the let-7a/Lin28B axis in ADS JZ SMCs. let-7a had a lower expression level in the 17β-estradiol ADS group (P<0.0001; Fig. 5A), while the expression level of Lin28B was higher in the 17β-estradiol ADS group compared with the ADS group (P<0.0001; Fig. 5B). These results indicated that 17β-estradiol may affect the expression of the let-7a/Lin28B axis to accelerate the progression of ADS.

Treatment with 17β-estradiol affects the let-7a/Lin28B axis in the proliferation of JZ SMCs. The lenti-GV369 cells had a higher proliferative ability when exposed to 17β-estradiol compared with the lenti-GV369 cells and the lenti-NC cells; there was a significant difference among the three groups (P<0.001; Fig. 6). These results indicated that 17β-estradiol promoted the let-7a/Lin28B axis to accelerate the proliferation of ADS.

Discussion

To the best of our knowledge, the present study demonstrated for first time that 17β-estradiol affects the expression level of the let-7a/Lin28B axis to accelerate the proliferation of JZ SMCs in ADS.

ADS is a common disease with diffuse, homogeneous, low-signal-intensity thickening of the JZ on MRI; when it is ≥12 mm, it is possible to diagnose ADS in combination with clinical symptoms (36). de Souza *et al* (37) found that

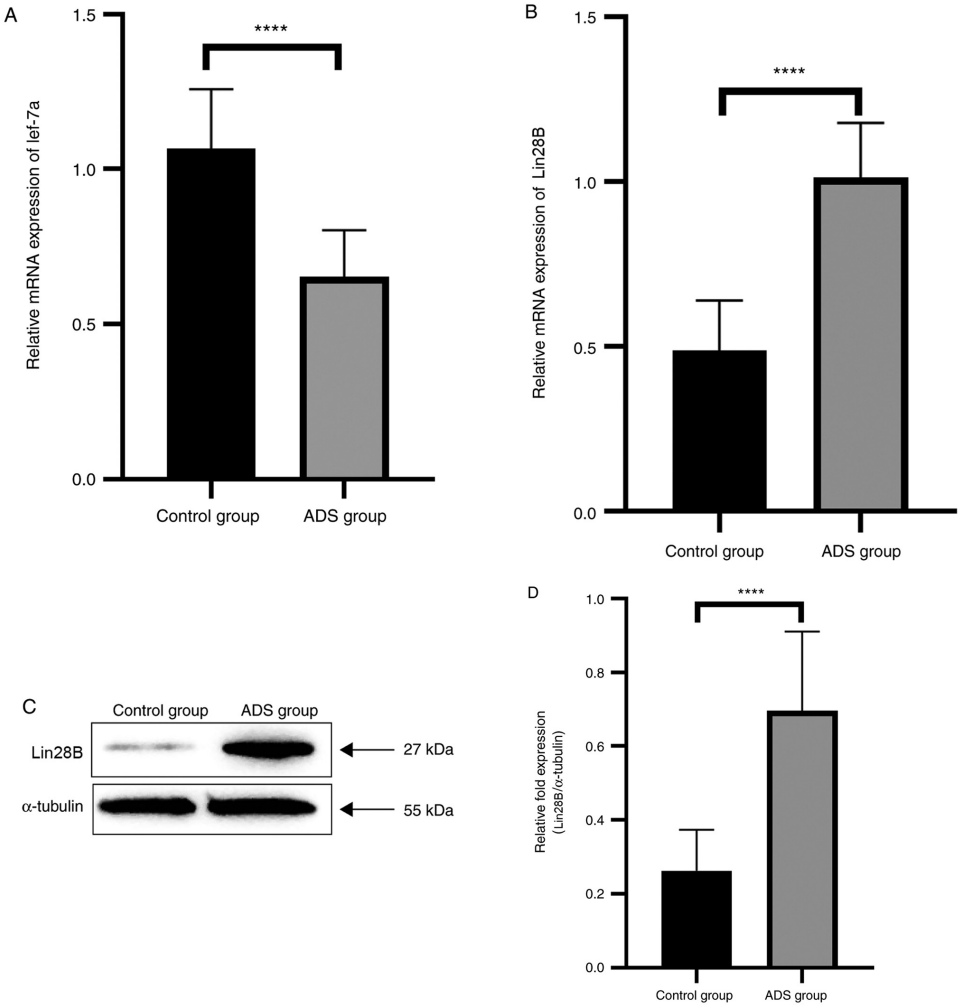

Figure 1. Expression levels of let-7a and Lin28B in junctional zone smooth muscle cells of the control group and the ADS group. (A) mRNA expression level of let-7a, as assessed via RT-qPCR, was normalized against that of U6 in the control group and the ADS group. (B) mRNA expression level of Lin28B, as assessed via RT-qPCR, was normalized against GAPDH in the control group and ADS group. (C) Protein expression level of Lin28B was determined using western blotting, and normalized against α-tubulin. (D) Relative fold expression of the Lin28B protein in the control group and the ADS group. These experiments were performed two times with three replicates in each experiment. Significance was determined via Student's t-test. ****P<0.0001. ADS, adenomyosis; RT-qPCR, reverse transcription-quantitative PCR.

subfertile patients with menorrhagia or dysmenorrhea had an incidence of 54% for JZ hyperplasia. In the histological diagnosis of ADS, hyperplastic bundles of SMCs surround the ectopic endometrial gland stroma, and although endometrial mucosal penetration is a general phenomenon, JZ thickening is much more extensive (38). In addition, high contraction waves are found to originate in the JZ of the non-pregnant uterus (9), and therefore, it is suggested that hyperplastic SMCs lead to the disruption of JZ architecture, further resulting in the initiation and development of ADS. The present study demonstrated that knockdown of let-7a could accelerate the proliferation of SMCs in the JZ. These findings preliminarily clarified that miRNAs participate in the development of ADS.

ADS is influenced by estrogens, and aromatase and estrogen sulfatase are highly expressed in ADS (1). Local hyperestrogenism is an important factor that accelerates the development of ADS. Some studies have shown that estrogen can induce the migration, invasion and angiogenesis of endometrial epithelial cells (39-41). Due to the common Müllerian origin, SMCs in JZs have some functional similarities with endometrial cells. For example, the expression levels of ER and progesterone receptor show cyclical changes in the JZ that are similar to that in the endometrium (42,43). Sun *et al* (15) noted that E2 induced enhanced proliferation in JZ SMCs in the ADS group via an ER-dependent pattern via the ras homolog gene family, member A/Rho-associated protein kinase signaling pathway. In addition, scholars have used the oral contraceptive pill or gonadotrophin-releasing hormone analogs to suppress ovarian activity and then observed an indistinct appearance of the myometrial layers in postmenopausal women on a MRI, while typical zonal anatomy reappeared in women treated with hormone replacement therapy (44). The present study also suggests that 17β-estradiol can accelerate the proliferation of ADS JZ SMCs by affecting the let-7a/Lin28B axis.

let-7a/Lin28B is a miRNA/protein axis that was first discovered in the nematode *Caenorhabditis elegans*, and has multiple functions in metastasis, tumorigenesis and cancer stem cell biology (24,45,46). let-7a has a low expression in numerous types of carcinomas, such as laryngeal squamous cell carcinoma (47), gastric carcinoma (48), colorectal carcinoma (49) and oral squamous cell carcinoma (50). The present results are in accordance with this regulatory mechanism, and the

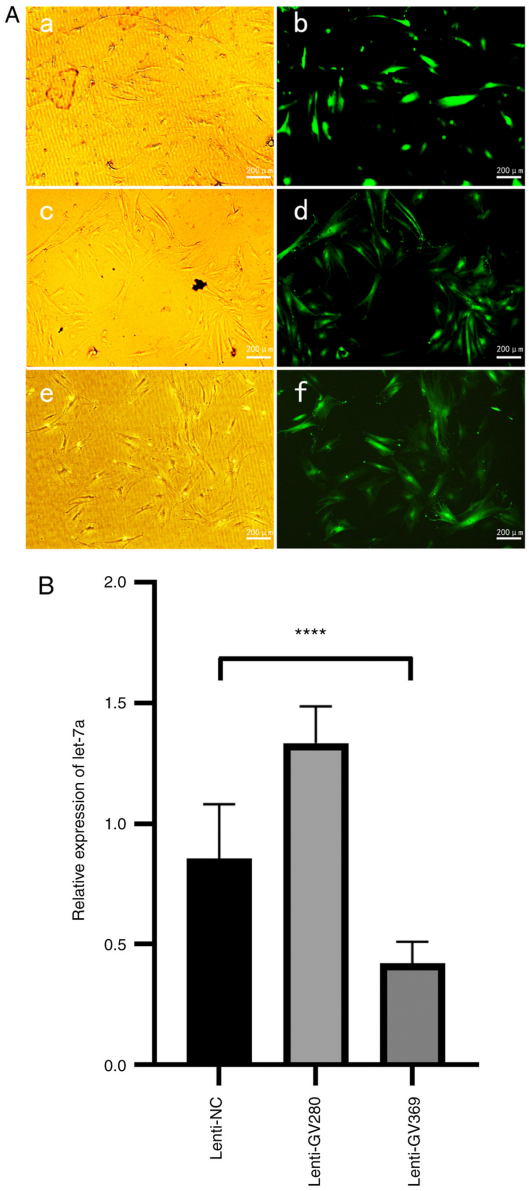

Figure 2. Transfection efficiency of let-7a lenti-vectors in junctional zone smooth muscle cells of the ADS group. (A) Cells were transfected with the lenti-null vector, let-7a overexpression lenti-vector GV280 and let-7a inhibition lenti-vector GV369 for 72 h, and transfection efficiency was observed using white light microscopy and fluorescence microscopy. Cells transfected with the lenti-null vector under (A-a) white light microscopy and (A-b) under fluorescence microscopy. Cells transfected with the let-7a overexpression lenti-vector GV280 under (A-c) white light microscopy and (A-d) fluorescence microscopy. Cells transfected with the let-7a inhibition lenti-vector GV369 under (A-e) white light microscopy and (A-f) fluorescence microscopy. Scale bar, 200 μm. (B) At 72 h post-infection, the cells were harvested, total RNA was isolated, and let-7a mRNA was quantified via reverse transcription-quantitative PCR and normalized against U6 in the ADS group. These experiments were performed two times with three replicates in each experiment. Significance was determined using one-way ANOVA. ****P<0.0001. ADS, adenomyosis; NC, negative control; lenti-, lentivirus.

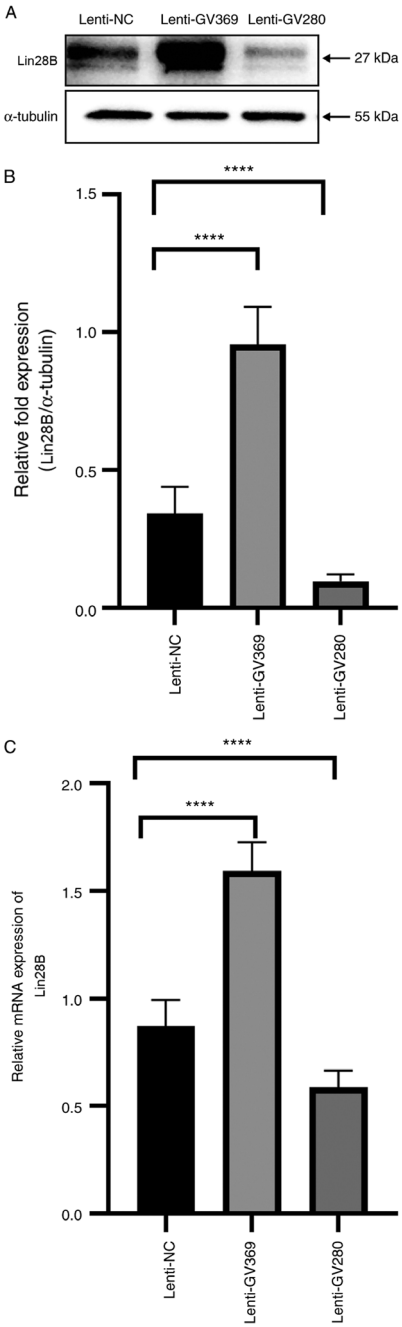

Figure 3. Expression level of Lin28B in junctional zone smooth muscle cells of the ADS group. (A) Cells in the ADS group were transfected with the lenti-null vector, let-7a inhibition lenti-vector GV369 and let-7a overexpression lenti-vector GV280 for 72 h, and then used for western blotting. (B) Relative expression protein level of Lin28B was normalized against α-tubulin in different let-7a-expressing ADS groups. (C) mRNA expression level of Lin28B was determined via reverse transcription-quantitative PCR and normalized against GAPDH in the different let-7a-expressing ADS groups. These experiments were performed two times with three replicates in each experiment. Significance was determined using one-way ANOVA. ****P<0.0001. ADS, adenomyosis; NC, negative control; lenti-, lentivirus.

expression level of let-7a was lower in the ADS group compared with in the control group. When let-7a was upregulated, the proliferation of the lenti-GV280 cells was inhibited. Lin28B is an RNA-binding protein that controls post-transcriptional processes, and has an opposite expression pattern in embryos and adults (51). Interestingly, it has been reported that Lin28B is upregulated in various cancer types (52-54). The present study identified that Lin28B was upregulated in the ADS group compared with the control group, and its expression level was negatively correlated with let-7a in JZ SMCs in ADS.

Although ADS is a common gynecological disease, its pathogenesis remains a difficult problem to solve, and there are several related theories. In addition to the invagination and metaplasia theories (55), the tissue injury and repair (TIAR) theory (20)

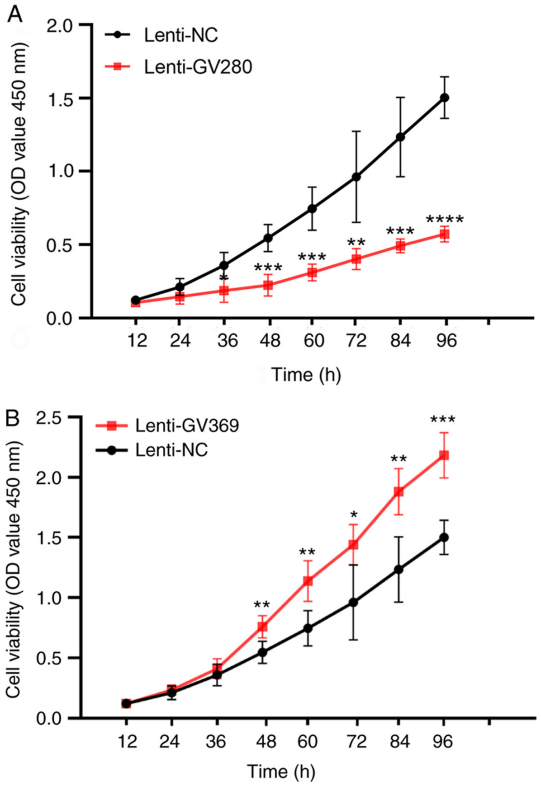

Figure 4. Proliferation of junctional zone smooth muscle cells in the ADS group. Cells were transfected with the lenti-null vector, let-7a inhibition lenti-vector GV369 and let-7a overexpression lenti-vector GV280 for 72 h, and then plated in 96-well plates at 1,000 cells/well density and incubated at 37˚C in 5% CO_2 for 12, 24, 36 48, 60, 72, 84 and 96 h. Cell Counting Kit-8 solution (10 μl) was added to each well at different times and incubated for 4 h. Finally, the 450 nm absorbance value was measured on a microplate reader. (A) The 450 nm absorbance between the cells transfected with lenti-NC and lenti-GV280 in the ADS group. (B) The 450 nm absorbance between the cells transfected with lenti-NC and lenti-GV369 in the ADS group. These experiments were performed two times with three replicates in each experiment. Significance was determined using a Student's t-test. *P<0.05, **P<0.01, ***P<0.001, ****P<0.0001 vs. Lenti-NC. lenti-, lentivirus; ADS, adenomyosis; NC, negative control; OD, optical density.

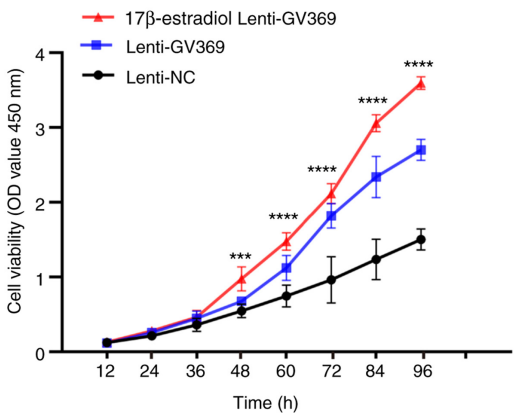

Figure 5. Proliferation of junctional zone smooth muscle cells of the 17β-estradiol- and let-7a inhibition lenti-vector GV369-treated ADS group and control group. Cells were transfected with the lenti-null vector or let-7a inhibition lenti-vector GV369 for 72 h, and then, some starved lenti-GV369 cells were exposed to 17β-estradiol for 24 h. Then, the 450 nm absorbance was tested in the 17β-estradiol lenti-GV369 group, lenti-GV369 group and lenti-NC group. These experiments were performed two times with three replicates in each experiment. Significance was determined via one-way ANOVA. There was significant difference among the three groups. ***P<0.001, ****P<0.0001. lenti-, lentivirus; ADS, adenomyosis; NC, negative control; OD, optical density.

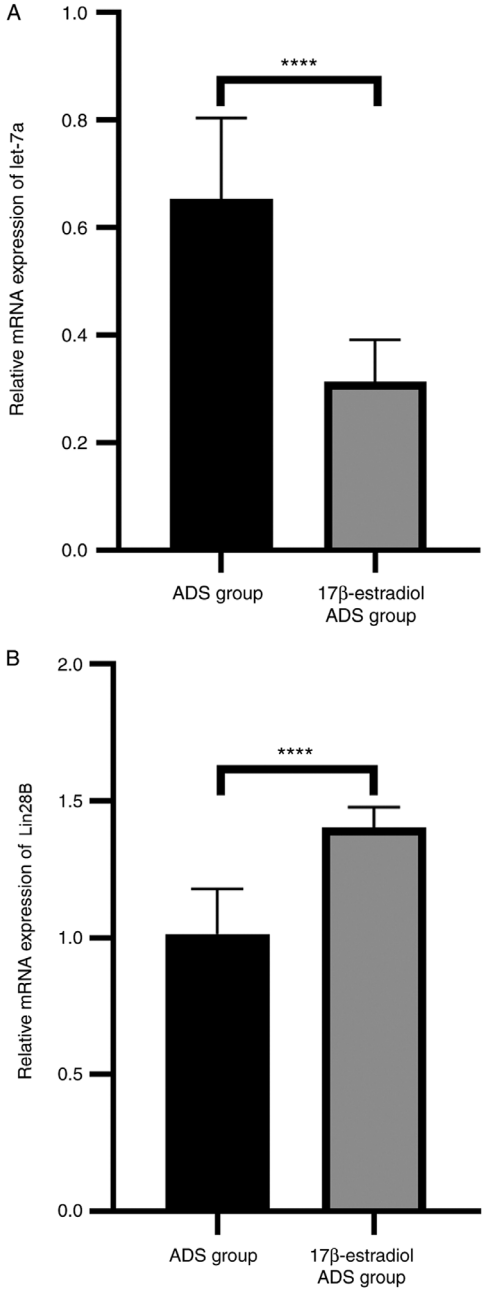

Figure 6. Expression levels of let-7a and Lin28B in junctional zone smooth muscle cells from the 17β-estradiol-treated ADS group and the control group. Cells in the starved state were exposed to 17β-estradiol for 24 h. (A) Relative mRNA expression of let-7a in the 17β-estradiol-treated ADS group and the control group. (B) Relative mRNA expression of Lin28B in the 17β-estradiol-treated ADS group and the control group. These experiments were performed two times with three replicates in each experiment. Significance was determined using a Student's t-test. ****P<0.0001. ADS, adenomyosis

suggests that endometrial-myometrial interface (EMI) microtraumatization causes tissue injury, which subsequently upregulates COX-2 and PGE2, ultimately resulting in increased local estrogen production. Then, elevated estrogen activates both ERα and ERβ, leading to the induction of OT/OTR signaling and subsequent increases in uterine peristalsis, angiogenesis and proliferation. The increased peristalsis could further exacerbate uterine hyperperistalsis, and thus, induce TIAR, causing endometrial invagination and ultimately the formation of adenomyotic lesions (18). The EMI disruption theory (4) is a revamp of the TIAR theory, which

accounts for the genesis of ADS arising from iatrogenic trauma such as dilatation and curettage procedures. Iatrogenic procedures or uterine hyperperistalsis cause EMI disruption, which leads to tissue hypoxia and activates TGF-β1, VEGF, platelet-derived growth factor, COX-2 and stromal cell-derived factor 1 signaling pathways, leading to enhanced uterine peristalsis, invasion of endometrial epithelial cells and ultimately the formation of adenomyotic lesions in the myometrium (4). All these theories suggest that ADS is a complicated and multipathogenic disease. Herndon *et al* (56) identified 1,024 aberrantly expressed genes, 140 upregulated and 884 downregulated genes, in ADS via microarray analysis. These genes participate in numerous cell functions and signaling pathways, such as apoptosis, extracellular matrix remodeling, oxidative phosphorylation and mitochondrial dysfunction. Moreover, the present study preliminarily demonstrated that miRNAs can control the development of ADS from the perspective of non-coding RNAs, and endocrine molecules can affect this process.

There are still some limitations in the present study. First, the current study only observed the SMCs in the JZ of ADS samples. Second, no further investigations were performed to determine whether let-7a affects the apoptosis of JZ SMCs in ADS. Third, for the purpose of minimizing variability, although the posterior uterine wall is the common place where ADS occurs (57-60), samples were collected from the anterior fundal wall. In addition, previous studies have shown that circular RNAs (circRNAs) act as miRNA sponges and that the circRNA-miRNA-mRNA network may have effects on cancer-related pathways (61-63), which the present study did not examine. Therefore, further cell functional experiments could help to elucidate the pathogenesis of ADS based on this point of view.

In conclusion, the present study demonstrated that let-7a was downregulated, whereas Lin28B was upregulated in ADS. In addition, let-7a could affect the expression levels of Lin28B; low expression of let-7a resulted in high Lin28B expression and high proliferation of JZ SMCs. Treatment with 17β-estradiol also affected the expression of the let-7a/Lin28B axis and the effects of this axis on the proliferation of JZ SMCs in ADS. Notably, 17β-estradiol and let-7a/Lin28B axis synergistically induced the higher proliferation of JZ SMCs in ADS.

Acknowledgements

Not applicable.

Funding

This work was funded by National Natural Science Foundation of China (grant no. 81571412).

Availability of data and materials

All data generated or analyzed during this study are included in this published article.

Authors' contributions

JHH drafted the manuscript, completed the experiments and performed statistical analysis. HD designed the experiment and revised the article. SW and YYW helped with collection of tissue samples, acquisition of data and interpretation of data. HD and SW confirm the authenticity of all the raw data. All authors read and approved the final manuscript.

Ethics approval and consent to participate

This study was approved by the Ethical Committee of Clinical Research of Beijing Obstetrics and Gynecology Hospital, Capital Medical University, China (reference no. 2016-KY-012), and conducted according to the Declaration of Helsinki. All patients signed informed consent before the hysterectomy.

Patient consent for publication

Not applicable.

Competing interests

The authors declare that they have no competing interests.

References

1. Kitawaki J: Adenomyosis: The pathophysiology of an oestrogen-dependent disease. Best Pract Res Clin Obstet Gynaecol 20: 493-502, 2006.
2. Yu O, Schulze-Rath R, Grafton J, Hansen K, Scholes D and Reed SD: Adenomyosis incidence, prevalence and treatment: United States population-based study 2006-2015. Am J Obstet Gynecol 223: 94.e1-94.e10, 2020.
3. Bird CC, McElin TW and Manalo-Estrella P: The elusive adenomyosis of the uterus - revisited. Am J Obstet Gynecol 112: 583-593, 1972.
4. Guo SW: The pathogenesis of adenomyosis vis-à-vis endometriosis. J Clin Med 9: 485, 2020.
5. O'Shea A, Figueiredo G and Lee SI: Imaging diagnosis of adenomyosis. Semin Reprod Med 38: 119-128, 2020.
6. Brosens JJ, de Souza NM and Barker FG: Uterine junctional zone: Function and disease. Lancet 346: 558-560, 1995.
7. Curtis KM, Hillis SD, Marchbanks PA and Peterson HB: Disruption of the endometrial-myometrial border during pregnancy as a risk factor for adenomyosis. Am J Obstet Gynecol 187: 543-544, 2002.
8. Guo SW, Mao X, Ma Q and Liu X: Dysmenorrhea and its severity are associated with increased uterine contractility and overexpression of oxytocin receptor (OTR) in women with symptomatic adenomyosis. Fertil Steril 99: 231-240, 2013.
9. Fusi L, Cloke B and Brosens JJ: The uterine junctional zone. Best Pract Res Clin Obstet Gynaecol 20: 479-491, 2006.
10. Tanos V, Lingwood L and Balami S: Junctional zone endometrium morphological characteristics and functionality: Review of the literature. Gynecol Obstet Invest 85: 107-117, 2020.
11. Imaoka I, Ascher SM, Sugimura K, Takahashi K, Li H, Cuomo F, Simon J and Arnold LL: MR imaging of diffuse adenomyosis changes after GnRH analog therapy. J Magn Reson Imaging 15: 285-290, 2002.
12. Khan KN, Kitajima M, Hiraki K, Fujishita A, Nakashima M, Ishimaru T and Masuzaki H: Cell proliferation effect of GnRH agonist on pathological lesions of women with endometriosis, adenomyosis and uterine myoma. Hum Reprod 25: 2878-2890, 2010.
13. Zhang Y, Zhou L, Li TC, Duan H, Yu P and Wang HY: Ultrastructural features of endometrial-myometrial interface and its alteration in adenomyosis. Int J Clin Exp Pathol 7: 1469-1477, 2014.
14. Wang S, Duan H, Zhang Y and Sun FQ: Abnormal activation of RhoA/ROCK-I signaling in junctional zone smooth muscle cells of patients with adenomyosis. Reprod Sci 23: 333-341, 2016.
15. Sun FQ, Duan H, Wang S and Li JJ; FQ S: 17β-estradiol induces overproliferation in adenomyotic human uterine smooth muscle cells of the junctional zone through hyperactivation of the estrogen receptor-enhanced RhoA/ROCK signaling pathway. Reprod Sci 22: 1436-1444, 2015.
16. Leyendecker G, Kunz G, Wildt L, Beil D and Deininger H: Uterine hyperperistalsis and dysperistalsis as dysfunctions of the mechanism of rapid sperm transport in patients with endometriosis and infertility. Hum Reprod 11: 1542-1551, 1996.

17. Kunz G, Noe M, Herbertz M and Leyendecker G: Uterine peristalsis during the follicular phase of the menstrual cycle: Effects of oestrogen, antioestrogen and oxytocin. Hum Reprod Update 4: 647-654, 1998.
18. Leyendecker G and Wildt L: A new concept of endometriosis and adenomyosis: Tissue injury and repair (TIAR). Horm Mol Biol Clin Investig 5: 125-142, 2011.
19. Liu X, Zou H, Zhao Y, Chen H, Liu T, Wu Z, Yang C, Li Q and Li Y: Tanshinone inhibits NSCLC by downregulating AURKA through Let-7a-5p. Front Genet 11: 838, 2020.
20. Leyendecker G, Wildt L and Mall G: The pathophysiology of endometriosis and adenomyosis: Tissue injury and repair. Arch Gynecol Obstet 280: 529-538, 2009.
21. Reinhart BJ, Slack FJ, Basson M, Pasquinelli AE, Bettinger JC, Rougvie AE, Horvitz HR and Ruvkun G: The 21-nucleotide let-7 RNA regulates developmental timing in *Caenorhabditis elegans*. Nature 403: 901-906, 2000.
22. Jiang J, Lee EJ, Gusev Y and Schmittgen TD: Real-time expression profiling of microRNA precursors in human cancer cell lines. Nucleic Acids Res 33: 5394-5403, 2005.
23. Jiang S and Baltimore D: RNA-binding protein Lin28 in cancer and immunity. Cancer Lett 375: 108-113, 2016.
24. Balzeau J, Menezes MR, Cao S and Hagan JP: The LIN28/let-7 Pathway in Cancer. Front Genet 8: 31, 2017.
25. Shyh-Chang N and Daley GQ; N S: Lin28: Primal regulator of growth and metabolism in stem cells. Cell Stem Cell 12: 395-406, 2013.
26. Hikasa H, Sekido Y and Suzuki A; H H: Merlin/NF2-Lin28B-let-7 is a tumor-suppressive pathway that is cell-density dependent and hippo independent. Cell Rep 14: 2950-2961, 2016.
27. Farzaneh M, Attari F and Khoshnam SE: Concise review: LIN28/let-7 signaling, a critical double-negative feedback loop during pluripotency, reprogramming, and tumorigenicity. Cell Reprogram 19: 289-293, 2017.
28. Shamsuzzama LK, Kumar L, Haque R and Nazir A: Role of MicroRNA Let-7 in modulating multifactorial aspect of neurodegenerative diseases: An Overview. Mol Neurobiol 53: 2787-2793, 2016.
29. Chien CS, Wang ML, Chu PY, Chang YL, Liu WH, Yu CC, Lan YT, Huang PI, Lee YY, Chen YW, *et al*: Lin28B/Let-7 regulates expression of Oct4 and Sox2 and reprograms oral squamous cell carcinoma cells to a stem-like state. Cancer Res 75: 2553-2565, 2015.
30. Peng F, Li TT, Wang KL, Xiao GQ, Wang JH, Zhao HD, Kang ZJ, Fan WJ, Zhu LL, Li M, *et al*: H19/let-7/LIN28 reciprocal negative regulatory circuit promotes breast cancer stem cell maintenance. Cell Death Dis 8: e2569, 2017.
31. Yin J, Zhao J, Hu W, Yang G, Yu H, Wang R, Wang L, Zhang G, Fu W, Dai L, *et al*: Disturbance of the let-7/LIN28 double-negative feedback loop is associated with radio- and chemo-resistance in non-small cell lung cancer. PLoS One 12: e0172787, 2017.
32. Cho S, Mutlu L, Grechukhina O and Taylor HS: Circulating microRNAs as potential biomarkers for endometriosis. Fertil Steril 103: 1252-60.e1, 2015.
33. Cho S, Mutlu L, Zhou Y and Taylor HS: Aromatase inhibitor regulates let-7 expression and let-7f-induced cell migration in endometrial cells from women with endometriosis. Fertil Steril 106: 673-680, 2016.
34. Lin SL, Duan H, Wang S and Li JJ; SL L: Overexpression of Lin28B promoted the proliferation of adenomyotic smooth muscle cells of the junctional zone via regulating Let-7a. Reprod Sci 27: 1156-1163, 2020.
35. Schmittgen TD and Livak KJ: Analyzing real-time PCR data by the comparative C(T) method. Nat Protoc 3: 1101-1108, 2008.
36. Reinhold C, McCarthy S, Bret PM, Mehio A, Atri M, Zakarian R, Glaude Y, Liang L and Seymour RJ: Diffuse adenomyosis: Comparison of endovaginal US and MR imaging with histopathologic correlation. Radiology 199: 151-158, 1996.
37. de Souza NM, Brosens JJ, Schwieso JE, Paraschos T and Winston RM: The potential value of magnetic resonance imaging in infertility. Clin Radiol 50: 75-79, 1995.
38. Reinhold C, Tafazoli F, Mehio A, Wang L, Atri M, Siegelman ES and Rohoman L: Uterine adenomyosis: Endovaginal US and MR imaging features with histopathologic correlation. Radiographics 19 (Suppl 1): S147-S160, 1999.
39. Benagiano G, Brosens I and Habiba M: Structural and molecular features of the endomyometrium in endometriosis and adenomyosis. Hum Reprod Update 20: 386-402, 2014.
40. Chen YJ, Li HY, Huang CH, Twu NF, Yen MS, Wang PH, Chou TY, Liu YN, Chao KC and Yang MH: Oestrogen-induced epithelial-mesenchymal transition of endometrial epithelial cells contributes to the development of adenomyosis. J Pathol 222: 261-270, 2010.
41. Huang TS, Chen YJ, Chou TY, Chen CY, Li HY, Huang BS, Tsai HW, Lan HY, Chang CH, Twu NF, *et al*: Oestrogen-induced angiogenesis promotes adenomyosis by activating the Slug-VEGF axis in endometrial epithelial cells. J Cell Mol Med 18: 1358-1371, 2014.
42. Daels J: Uterine contractility patterns of the outer and inner zones of the myometrium. Obstet Gynecol 44: 315-326, 1974.
43. Brosens JJ, Barker FG and de Souza NM: Myometrial zonal differentiation and uterine junctional zone hyperplasia in the non-pregnant uterus. Hum Reprod Update 4: 496-502, 1998.
44. McCarthy S, Tauber C and Gore J: Female pelvic anatomy: MR assessment of variations during the menstrual cycle and with use of oral contraceptives. Radiology 160: 119-123, 1986.
45. Slack FJ, Basson M, Liu Z, Ambros V, Horvitz HR and Ruvkun G: The lin-41 RBCC gene acts in the *C. elegans* heterochronic pathway between the let-7 regulatory RNA and the LIN-29 transcription factor. Mol Cell 5: 659-669, 2000.
46. Moss EG, Lee RC and Ambros V: The cold shock domain protein LIN-28 controls developmental timing in *C. elegans* and is regulated by the lin-4 RNA. Cell 88: 637-646, 1997.
47. Luo C, Zhang J, Zhang Y, Zhang X, Chen Y and Fan W: Low expression of miR-let-7a promotes cell growth and invasion through the regulation of c-Myc in oral squamous cell carcinoma. Cell Cycle 19: 1983-1993, 2020.
48. Yang Q, Jie Z, Cao H, Greenlee AR, Yang C, Zou F and Jiang Y: Low-level expression of let-7a in gastric cancer and its involvement in tumorigenesis by targeting RAB40C. Carcinogenesis 32: 713-722, 2011.
49. Re M, Magliulo G, Gioacchini FM, Bajraktari A, Bertini A, Çeka A, Rubini C, Ferrante L, Procopio AD and Olivieri F: Expression levels and clinical significance of miR-21-5p, miR-let-7a, and miR-34c-5p in laryngeal squamous cell carcinoma. BioMed Res Int 2017: 3921258, 2017.
50. Liu TP, Huang CC, Yeh KT, Ke TW, Wei PL, Yang JR and Cheng YW: Down-regulation of let-7a-5p predicts lymph node metastasis and prognosis in colorectal cancer: Implications for chemotherapy. Surg Oncol 25: 429-434, 2016.
51. Viswanathan SR and Daley GQ; SR V: Lin28: A microRNA regulator with a macro role. Cell 140: 445-449, 2010.
52. King CE, Cuatrecasas M, Castells A, Sepulveda AR, Lee JS and Rustgi AK: LIN28B promotes colon cancer progression and metastasis. Cancer Res 71: 4260-4268, 2011.
53. West JA, Viswanathan SR, Yabuuchi A, Cunniff K, Takeuchi A, Park IH, Sero JE, Zhu H, Perez-Atayde A, Frazier AL, *et al*: A role for Lin28 in primordial germ-cell development and germ-cell malignancy. Nature 460: 909-913, 2009.
54. Zhou J, Ng SB and Chng WJ: LIN28/LIN28B: An emerging oncogenic driver in cancer stem cells. Int J Biochem Cell Biol 45: 973-978, 2013.
55. García-Solares J, Donnez J, Donnez O and Dolmans MM: Pathogenesis of uterine adenomyosis: Invagination or metaplasia? Fertil Steril 109: 371-379, 2018.
56. Herndon CN, Aghajanova L, Balayan S, Erikson D, Barragan F, Goldfien G, Vo KC, Hawkins S and Giudice LC: Global transcriptome abnormalities of the eutopic endometrium from women with adenomyosis. Reprod Sci 23: 1289-1303, 2016.
57. Mijatovic V, Florijn E, Halim N, Schats R and Hompes P: Adenomyosis has no adverse effects on IVF/ICSI outcomes in women with endometriosis treated with long-term pituitary down-regulation before IVF/ICSI. Eur J Obstet Gynecol Reprod Biol 151: 62-65, 2010.
58. Levgur M: Diagnosis of adenomyosis: A review. J Reprod Med 52: 177-193, 2007.
59. Halvorsen TB and Moen MH: The extent and clinical significance of adenomyotic lesions in the uterine wall. A quantitative assessment. APMIS 101: 907-913, 1993.
60. Bohlman ME, Ensor RE and Sanders RC: Sonographic findings in adenomyosis of the uterus. AJR Am J Roentgenol 148: 765-766, 1987.
61. Ma HB, Yao YN, Yu JJ, Chen XX and Li HF: Extensive profiling of circular RNAs and the potential regulatory role of circRNA-000284 in cell proliferation and invasion of cervical cancer via sponging miR-506. Am J Transl Res 10: 592-604, 2018.
62. Guo J, Chen M, Ai G, Mao W, Li H and Zhou J: Hsa_circ_0023404 enhances cervical cancer metastasis and chemoresistance through VEGFA and autophagy signaling by sponging miR-5047. Biomed Pharmacother 115: 108957, 2019.
63. Liu J, Wang D, Long Z, Liu J and Li W: CircRNA8924 promotes cervical cancer cell proliferation, migration and invasion by competitively binding to MiR-518d-5p/519-5p family and modulating the expression of CBX8. Cell Physiol Biochem 48: 173-184, 2018.